Bull. Mater. Sci., Vol. 33, No. 3, June 2010, pp. 227–231. © Indian Academy of Sciences.

Red luminescence from hydrothermally synthesized Eu-doped ZnO nanoparticles under visible excitation

P M ANEESH and M K JAYARAJ*

Department of Physics, Cochin University of Science and Technology, Kochi 682 022, India

MS received 16 May 2008; revised 9 February 2010

Abstract. **Eu-doped ZnO nanoparticles were synthesized by hydrothermal method. The Eu-dopant concentration has been varied by varying the amount of Eu-dopant concentration. These nanoparticles were structurally characterized by X-ray diffraction, transmission electron microscopy and selected area electron diffraction and it confirms the formation of nanoparticles having standard wurtzite structure. Photoluminescence studies show that these nanoparticles exhibit a sharp red luminescence due to the intra-4*f* transitions of Eu^{3+} ions at an excitation of 397 nm and 466 nm. Luminescence quenching is observed in the nanoparticles as the Eu-dopant concentration increases. Incorporation of Eu in the nanoparticles was confirmed by the energy dispersive X-ray studies.**

Keywords. **Zinc oxide; X-ray diffraction; transmission electron microscopy; photoluminescence; luminescence quenching.**

1. Introduction

Phosphor, which has high efficiency and low degradation, is required for the development of lighting technology and for flat panel displays such as field emission displays (FEDs) and plasma display panels (PDPs) (Blasse and Grabmaier 1994; Yen and Shionoya 1998). The use of oxide phosphors in place of conventional sulphide phosphors has been preferred for FED applications due to higher stability in high vacuum environment and less emission of contaminating gases (Itoh *et al* 1991).

High quality II–VI semiconductor nanocrystals and their luminescence properties have been studied recently both experimentally and theoretically (Murray *et al* 1993; Nirmal *et al* 1996; Empedocles *et al* 1996; Efros and Rosen 1997; Matsuura *et al* 2000). The II–VI semiconductor nanomaterials are unique host materials for doping of highly optically active impurities, and semiconductor doped with luminescence centres exhibit efficient luminescence even at room temperature (Bhargava *et al* 1994; Bol and Meijerink 1998).

In recent years, rare earth (RE) doped wide bandgap semicoducting nanomaterials have attracted wide use in various applications such as thin film electroluminescent (TFEL) devices (Kossanyi *et al* 1990), optoelectronic or cathodoluminescent devices (Leskela 1998). RE-doped insulators are used in telecommunications, lasers and amplifiers (Jacquier *et al* 2000), medical analysis and phosphors (Blasse and Grabmaier 1994), etc.

CdSe and CdS are the most widely studied among the II–VI semiconductor nanoparticles (Murray *et al* 1993; Brus *et al* 1996; Nirmal *et al* 1996; Empedocles *et al* 1996; Matsuura *et al* 2000; Peng *et al* 2000; Hu *et al* 2001). However, these materials contain toxic elements such as Cd and Se. Zinc oxide (ZnO) is a wide bandgap (3·3 eV) II–VI compound semiconductor with large exciton binding energy (60 meV) at room temperature. ZnO is an environmentally friendly material and is one of the suitable candidates for practical use as a nanodevice material. It has a stable wurtzite structure with lattice spacing, $a = 0{\cdot}325$ nm and $c = 0{\cdot}521$ nm. Most of the ZnO: RE^{3+} crystals have been synthesized by traditional high temperature solid state method (Kossanyi *et al* 1990; Kouyate *et al* 1991; Bachir *et al* 1996, 1997) which is energy consuming and difficult to control the particle properties.

Rare-earth (RE) ions are better luminescent centres than the transition metal elements because their 4*f* intrashell transitions originate at narrow and intense emission lines. In this paper, we report the synthesis of Eu-doped ZnO nanoparticles by low temperature hydrothermal method and their photoluminescence emission characteristics.

2. Experimental

The Eu-doped ZnO nanoparticles were synthesized from the stock solutions of $Zn(CH_3COO)_2{\cdot}2H_2O$ (0·1 M) prepared in 50 ml methanol under stirring. To this solution, Eu_2O_3 varying from 0·005–0·03 g was added. This led to europium concentration variation from 1·2–5·27 at.% in

*Author for correspondence (mkj@cusat.ac.in)

the ZnO nanoparticle. 25 ml of NaOH (0·3 M) solution prepared in methanol was mixed with the above solution under continuous stirring in order to get the pH of reactants between 8 and 11. These solutions were transferred into teflon lined sealed stainless steel autoclaves and maintained at 150°C for 12 h under autogenous pressure. It was then allowed to cool naturally to room temperature. After the reaction was complete, the resulting white solid products were washed with methanol, filtered and then dried in air in a laboratory oven at 60°C. The undoped ZnO nanoparticles were also synthesized in a similar manner described above but without adding Eu_2O_3.

The synthesized samples were characterized for their structure by X-ray diffraction (Rigaku D max-C) with CuKα radiation. Transmission electron microscopy (TEM), selected area electron diffraction (SAED) and high resolution transmission electron microscopy (HRTEM) were performed with a JEOL JEM-3100F transmission electron microscope operating at 200 kV. The sample for TEM was prepared by placing a drop of the ZnO suspension in methanol onto a standard carbon coated copper grid. The grids were dried before recording the micrographs. The elemental composition of the Eu-doped ZnO nanoparticles were determined using energy dispersive X-ray spectroscopy (EDX). Room temperature photoluminescence (PL) of the samples was measured on Horiba Jobin Yvon Fluoromax-3 spectrofluorimeter using Xe lamp as the excitation source.

3. Results and discussion

The X-ray diffraction data were recorded with CuKα radiation (1·5418 Å). The intensity data were collected over a 2θ range of 20–80°.

All the peaks in the X-ray diffraction pattern (figure 1) are assigned to the typical wurtzite structure of ZnO (ICSD Card No. 086254). There are no characteristic peaks of Eu_2O_3 regardless of the Eu-dopant concentration. Thus the wurtzite structure is not modified by the addition of Eu into the ZnO matrix. The average grain size (D) of the samples was estimated with the help of Scherrer equation using the diffraction intensity of (101) peak (Klug and Alexander 1954):

$$D = 0{\cdot}89\lambda/(\beta\cos\theta),$$

where λ is the X-ray wavelength, β the full width at half-maximum (FWHM) of the ZnO (101) line and θ the diffraction angle.

The broadening of the diffraction peaks is an indication that the synthesized materials are in nanometer regime. The grain size was found to be in the range of 9–12 nm depending on the growth condition. The lattice parameters calculated were also in agreement with the reported values.

EDX results show that the elemental percentage of the Eu ions incorporated in the Eu-doped ZnO nanoparticles are 1·2, 2·3, 4·53 and 5·27 at.% as 0·005, 0·01, 0·02 and 0·03 g Eu_2O_3 were used in the precursor solution.

Figure 2(a) shows TEM image and the corresponding SAED pattern of 2·3 at.% Eu-doped ZnO synthesized by hydrothermal method. TEM image confirms the formation of nanoparticles and it has an average size of 8 nm and they are spherical in shape. This result is consistent with what we had obtained from XRD analysis. From the diffraction rings in the SAED pattern, (002), (102) and (110) planes of ZnO were identified.

Figure 2(b) shows TEM image and the corresponding SAED pattern of 3·78 at.% Eu-doped ZnO by hydrothermal method. TEM image confirms the size of the particles to be in the nanoregime. These are not spherical in shape and it has a length of 20 nm and diameter of 7 nm. From the diffraction rings in the SAED pattern, (002), (102) and (110) planes of ZnO were identified.

Figure 3(a) shows the photoluminescent emission spectra of Eu-doped ZnO nanoparticles at an excitation wavelength (λ_{exc}) of 397 nm. The excitation energy almost coincides with the energy of $^7F_0 \rightarrow {}^5L_6$ transitions of Eu^{3+} ions, which is 3·147 eV (Peres *et al* 2007). Excitation at 397 nm yields the characteristic emissions of Eu^{3+} corresponding to ^5D_j (j = 0, 1) $\rightarrow {}^7F_j$ (j = 0, 1, 2, 3 and 4). The direct excitation of Eu^{3+} enhances the PL due to Eu^{3+} ions. The emission at 596 nm originates from the magnetic-dipole allowed $^5D_0 \rightarrow {}^7F_1$ transition, indicating that Eu^{3+} ions occupy a site with inversion symmetry and 617 nm from electric-dipole allowed $^5D_0 \rightarrow {}^7F_2$ transition, which results in a large transition probability in the crystal field with inversion antisymmetry. The intensity of emission corresponds to the $^5D_0 \rightarrow {}^7F_2$ transition which is stronger than that of $^5D_0 \rightarrow {}^7F_1$ transition. It is suggested that the

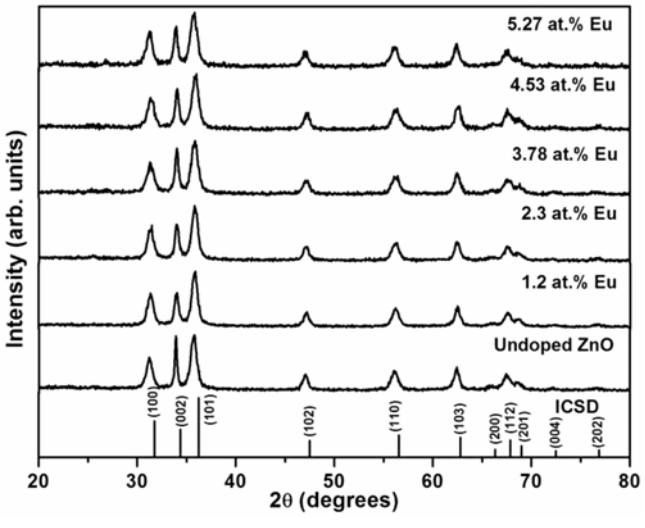

Figure 1. XRD pattern of undoped ZnO and Eu-doped ZnO nanoparticles of varying Eu dopant concentration.

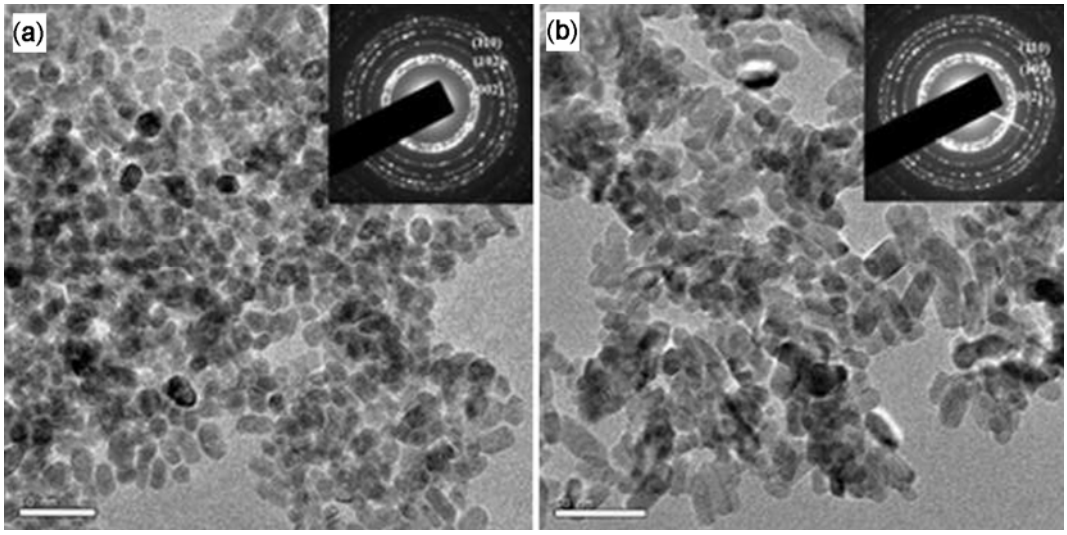

Figure 2. TEM image of Eu-doped ZnO nanoparticles with (**a**) 1·2 at.% and (**b**) 3·78 at.% Eu dopant concentration. SAED pattern of the ZnO : Eu with (**a**) 1·2 at.% and (**b**) 3·78 at.% Eu dopant concentration is in the inset.

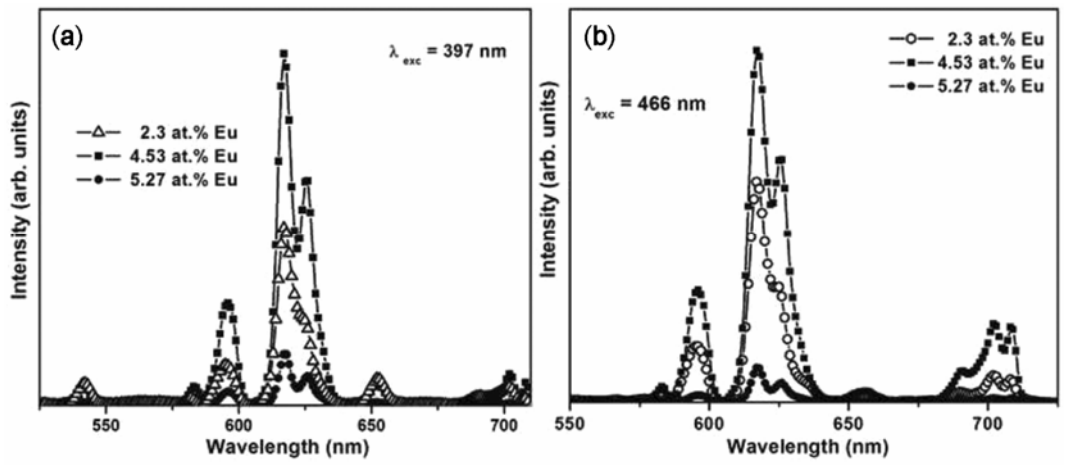

Figure 3. Room temperature photoluminescence emission spectra of Eu-doped ZnO nanoparticles excited for various Eu dopant concentrations at an excitation wavelength of (**a**) 397 nm and (**b**) 466 nm.

Eu^{3+} ions mainly take a site with inversion antisymmetry in the ZnO host. The emission at 701 nm is from $^5D_0 \rightarrow {}^7F_4$ transition and at 653 nm is from $^5D_0 \rightarrow {}^7F_3$ transition. The emission peaks at 583 nm corresponds to $^5D_0 \rightarrow {}^7F_0$ transition. The observation of forbidden $^5D_0 \rightarrow {}^7F_0$ transition indicates that some of the Eu ions are at low site symmetry. The emission at 543 nm is from $^5D_1 \rightarrow {}^7F_1$ transition.

The luminescent intensity of Eu-doped ZnO nanoparticles increases with increase in the Eu-dopant concentration at first and then it decreases. When the activator concentration increases above a certain level, luminescence begins to quench. Thus the emission intensity of $^5D_0 \rightarrow {}^7F_j$ (j = 0–4) depends on Eu-dopant concentration. In this case, the pairing or aggregation of activator atoms at high concentration may change a fraction of the activators into quenchers and induce the quenching effect. The migration of excitation by resonant energy transfer between the Eu^{3+} activators can sometimes be so efficient that it may carry the energy to a distant killer or to a quenching centre existing at the surface of the crystal.

Figure 3(b) shows the photoluminescent emission spectra of Eu-doped ZnO nanoparticles excited at 466 nm. The peaks at 583, 596, 617, 653 and 701 nm corresponding to the $^5D_0 \rightarrow {}^7F_j$ (j = 0–4) transitions of Eu^{3+} ions are dominated by the $^5D_0 \rightarrow {}^7F_2$ transition at 617 nm. In addition, the emission intensity increases with increasing Eu dopant concentration up to 4·53 at.% and then it decreases due to the concentration quenching.

Figure 4 shows the room temperature photoluminescence emission spectrum of the ZnO nanoparticles excited at 362 nm. Green emission at 545 nm was observed from

the hydrothermally synthesized ZnO nanoparticles. It can be attributed to the transition between singly charged oxygen vacancy and photo excited hole or Zn interstitial related defects (Vanheusden *et al* 1996; Peng *et al* 2006; Aneesh *et al* 2007). The inset in figure 4 shows the photoluminescent excitation spectra of the ZnO nanoparticles (λ_{em} = 545 nm) which indicates that the excitation is at 362 nm. The excitation peak corresponds to the band to band transition which shows a blue shift in the band-gap of ZnO nanoparticles.

Figure 5 shows the variation of PL integral intensity, at an excitation wavelength of 397 nm and 466 nm, as the Eu dopant concentration in ZnO increases from 1·2–5·27 at.%. The PL integral intensity increases with increasing amount of Eu dopant concentration up to 4·53 at.% and then it decreases due to the concentration quenching.

When the nanoparticles are excited with a wavelength of 325 nm, no intra-4f^6 Eu^{3+} related emission is observed. The disappearance of the red emission excited at 325 nm wavelength is probably related to the shielding effect due to the existence of the Eu_{Zn}* level (Yang *et al* 2006).

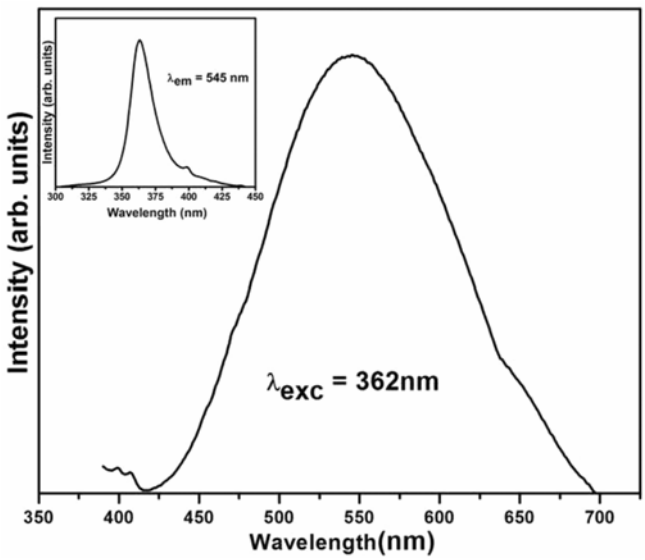

Figure 4. Room temperature photoluminescence spectra of ZnO nanoparticle excited at λ_{exc} = 362 nm. The inset shows the corresponding photoluminescent excitation spectra (λ_{em} = 545 nm) of ZnO nanoparticles.

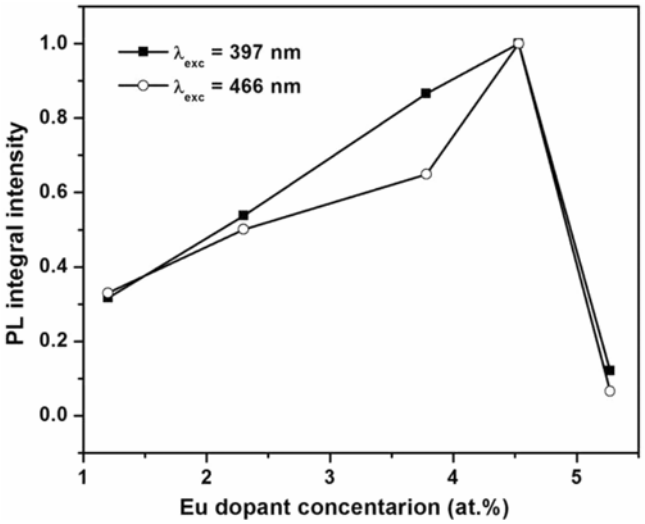

Figure 5. Variation of PL integral intensity with amount of Eu dopant concentration under 397 nm and 466 nm excitations.

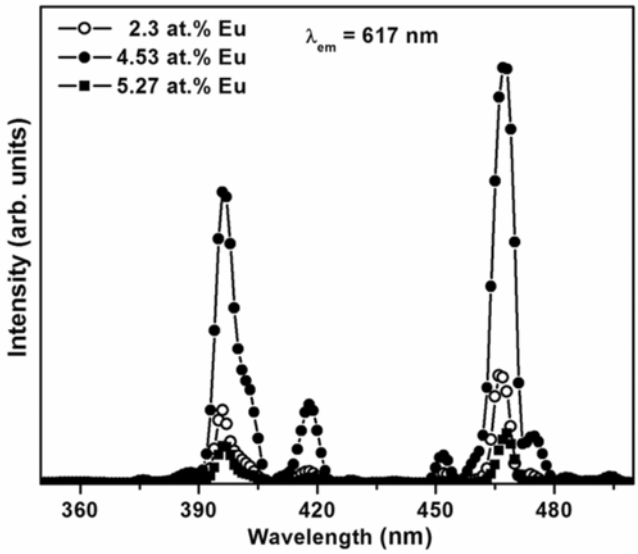

Figure 6. Room temperature photoluminescent excitation spectra of Eu-doped ZnO nanoparticles (λ_{em} = 617 nm).

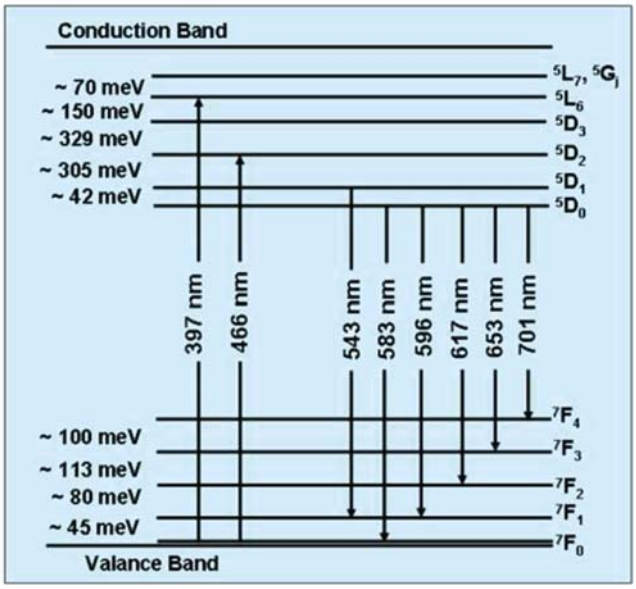

Figure 7. Simplified energy diagram of Eu^{3+} in Eu-doped ZnO nanoparticles. The energies of absorption and emission lines are also shown.

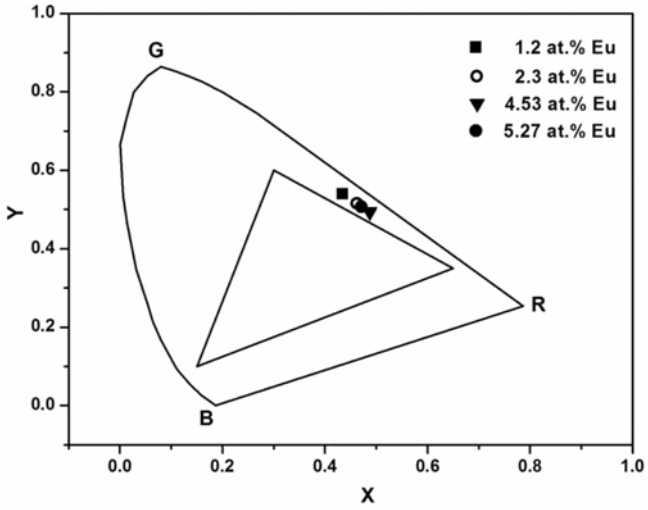

Figure 8. CIE diagram of Eu-doped ZnO nanoparticles synthesized by varying the Eu dopant concentration (1·2–5·27 at.%).

Thus 325 nm photon is not in resonance with any transitions of Eu^{3+} ions.

Figure 6 shows the photoluminescent excitation (PLE) spectra of the Eu-doped ZnO nanoparticles (λ_{em} = 617 nm) which indicates that the excitation is at 397 and 466 nm. The excitation peaks at 397 nm and 466 nm corresponds to the $^7F_0 \rightarrow {}^5L_6$ and $^7F_0 \rightarrow {}^5D_2$ transitions of Eu^{3+} ions. The peak at 418 nm corresponds to the $4F \rightarrow 5D$ transition of Eu^{2+} ion (Zhang *et al* 2007). It also shows that the PLE intensity increases with increase in the Eu dopant concentration up to 4·53 at.% and then it decreases. Figure 7 shows a schematic representation of the main energy levels identified in the studied samples (Peres *et al* 2007).

The CIE colour coordinates measured from the photoluminescent emission of Eu-doped ZnO nanoparticles by varying the Eu dopant concentration are shown in figure 8. For the case of the Eu-doped ZnO nanoparticles with Eu dopant concentration of 1·2 at.%, 2·3 at.%, 4·53 at.% and 5·27 at.%, the CIE coordinates are (0·43, 0·54), (0·46, 0·52), (0·49, 0·49) and (0·47, 0·51), respectively and these show the colors in yellowish–orange and yellow regions.

4. Conclusions

Europium doped ZnO nanoparticles were synthesized by hydrothermal method by varying the Eu dopant concentration. XRD and SAED results show these nanoparticles have wurtzite structure and the particle size distributions were studied from the TEM. The red PL emissions from the intra-4*f* transition of Eu^{3+} ions are observed under an excitation of 397 and 466 nm. Luminescence quenching is observed in the nanoparticles as the Eu-dopant concentration increases. Incorporation of Eu in the nanoparticles was confirmed by EDX studies.

Acknowledgements

The work is supported by the Department of Science and Technology, Government of India, under nanoscience and technology initiative. The authors thank the Sophisticated Analysis Instrument Facility Centre, IIT Chennai, for TEM measurements. One of the authors (PMA) thanks the Kerala State Council for Science, Technology and Environment for the award of a research fellowship.

References

Aneesh P M, Vanaja K A and Jayaraj M K 2007 *Proc. SPIE* **6639** 6690J

Bachir S, Azuma K, Kossanyi J, Valat P and Ronfard-Haret J C 1997 *J. Luminesc.* **75** 35

Bachir S, Sandouly C, Kossanyi J and Ronfard-Haret J C 1996 *J. Phys. Chem. Solids* **57** 1869

Bhargava R N, Gallagher D, Hong X and Nurmikko A 1994 *Phys. Rev. Lett.* **72** 416

Blasse G and Grabmaier B C 1994 *Luminescent materials* (New York: Springer)

Bol A A and Meijerink A 1998 *Phys. Rev.* **B58** R15997

Brus L E, Efros Al L and Itoh T 1996 *J. Lumin.* **70** 1

Efros Al L and Rosen M 1997 *Phys. Rev. Lett.* **78** 1110

Empedocles S A, Norris D J and Bawendi M G 1996 *Phys. Rev. Lett.* **77** 3873

Hu J, Li L S, Yang W, Manna L, Wang L W and Alivisatos A P 2001 *Science* **292** 2060

Itoh S, Toki H, Sato Y, Morimoto K and Kishino T 1991 *J. Electrochem. Soc.* **138** 1509

Jacquier B, Lebrasseur E, Guy S, Belarouci A and Menchini F 2000 *J. Alloys Compds.* **303** 207

ICSD Card No. 086254

Klug H P and Alexander L E 1954 *X-ray diffraction: Procedures for polycrystalline and amorphous materials* (New York: Wiley) 1st edn, Ch. 9

Kossanyi J *et al* 1990 *J. Lumin.* **46** 17

Kouyate D, Ronfard-Haret J C and Kossanyi J 1991 *J. Lumin.* **50** 205

Leskela M 1998 *J. Alloys Compds.* **275** 702

Matsuura D, Kanemitsu Y, Kushida T, White C W, Budai J D and Meldrum A 2000 *Appl. Phys. Lett.* **77** 2289

Murray C B, Norris D J and Bawendi M G 1993 *J. Am. Chem. Soc.* **115** 8706

Nirmal N, Dabbousi B O, Bawendi M G, Macklin J I, Trautman J K, Harris T D and Brus L E 1996 *Nature* (*London*) **383** 802

Peng X, Manna L, Yang W, Wickham J, Scher E, Kadavanich A and Alivisatos A P 2000 *Nature* (*London*) **404** 59

Peng W Q, Qu S C, Cong G W and Wang Z G 2006 *Mater. Sci. Semicond. Process.* **9** 156

Peres M *et al* 2007 *Appl. Phys.* **A88** 129

Vanheusden K, Warren W L, Seager C H, Tallant D R, Voigt J A and Gnade B E 1996 *J. Appl. Phys.* **79** 7983

Yang C C, Cheng S Y, Lee H Y and Chen S Y 2006 *Ceram. Int.* **32** 37

Yen W M and Shionoya S (eds) 1998 *Phosphor handbook* (Boca Raton, FL: CRC Press)

Zhang X, Wang J, Zhang J and Su Q 2007 *Mater. Lett.* **61** 761